HHS Public Access

Author manuscript

Obesity (Silver Spring). Author manuscript; available in PMC 2018 September 25.

Published in final edited form as:

Obesity (Silver Spring). 2010 August ; 18(8): 1493–1502. doi:10.1038/oby.2009.456.

Respiration in Adipocytes is Inhibited by Reactive Oxygen Species

Tong Wang[1], **Yaguang Si**[1], **Orian S. Shirihai**[1], **Huiqing Si**[1], **Vera Schultz**[1], **Richard F. Corkey**[1], **Liping Hu**[1], **Jude T. Deeney**[1], **Wen Guo**[1], and **Barbara E. Corkey**[1]

[1]Obesity Research Center, Department of Medicine, Boston University School of Medicine, Boston, Massachusetts, USA

Abstract

It is a desirable goal to stimulate fuel oxidation in adipocytes and shift the balance toward less fuel storage and more burning. To understand this regulatory process, respiration was measured in primary rat adipocytes, mitochondria, and fat-fed mice. Maximum O_2 consumption, *in vitro*, was determined with a chemical uncoupler of oxidative phosphorylation (carbonylcyanide p-trifluoromethoxyphenylhydrazone (FCCP)). The adenosine triphosphate/adenosine diphosphate (ATP/ADP) ratio was measured by luminescence. Mitochondria were localized by confocal microscopy with MitoTracker Green and their membrane potential ($\Delta\Psi_M$) measured using tetramethylrhodamine ethyl ester perchlorate (TMRE). The effect of N-acetylcysteine (NAC) on respiration and body composition *in vivo* was assessed in mice. Addition of FCCP collapsed $\Delta\Psi_M$ and decreased the ATP/ADP ratio. However, we demonstrated the same rate of adipocyte O_2 consumption in the absence or presence of fuels and FCCP. Respiration was only stimulated when reactive oxygen species (ROS) were scavenged by pyruvate or NAC: other fuels or fuel combinations had little effect. Importantly, the ROS scavenging role of pyruvate was not affected by rotenone, an inhibitor of mitochondrial complex I. In addition, mice that consumed NAC exhibited increased O_2 consumption and decreased body fat *in vivo*. These studies suggest for the first time that adipocyte O_2 consumption may be inhibited by ROS, because pyruvate and NAC stimulated respiration. ROS inhibition of O_2 consumption may explain the difficulty to identify effective strategies to increase fat burning in adipocytes. Stimulating fuel oxidation in adipocytes by decreasing ROS may provide a novel means to shift the balance from fuel storage to fuel burning.

INTRODUCTION

The main fate of the fuels, glucose, and fatty acids (FAs), in adipocytes is utilization for synthesis of triglycerides (TGs). However, the mechanism responsible for low rates of partitioning toward oxidation is not known. The ability to regulate FA partitioning away

Correspondence: Barbara E. Corkey (bcorkey@bu.edu).

The first two authors contributed equally to this work.

SUPPLEMENTARY MATERIAL

Supplementary material is linked to the online version of the paper at http://www.nature.com/oby

DISCLOSURE

The authors declared no conflict of interest.

from storage toward oxidation could be valuable in controlling obesity. Our studies are directed at elucidating control of FA oxidation. We expect that understanding FA partitioning could lead to identification of a direct cause of obesity and putative targets to promote its prevention.

The fate of FA in cells is mainly regulated by three enzymes: acyl-CoA synthetase, which activates FA to the cellular metabolite, long-chain acyl CoA (LC-CoA); carnitine palmitoyl transferase-1, the gatekeeper of FA entry into the mitochondria for oxidation, and acetyl CoA carboxylase; the generator of malonyl-CoA that regulates carnitine palmitoyl transferase-1 activity. The initial step in FA metabolism toward either TG synthesis or oxidation is activation by acyl-CoA synthetase to form LC-CoA. It is generally accepted that the partitioning of LC-CoA between oxidation and storage is determined by whether carnitine palmitoyl transferase-1 is activated to favor oxidation or inhibited by malonyl-CoA to favor synthesis (1). Our prior studies evaluating the expression and activity of these three enzymes of partitioning do not explain a low rate of FA oxidation in adipocytes (2–4).

Mitochondria and oxidative phosphorylation are important to adipocytes. As preadipocytes undergo adipogenesis there is a 20- to 30-fold increase in mitochondrial number in the cell and in the concentration of numerous mitochondrial proteins (5,6) accompanied by increased O_2 consumption (7). Thiazolidinediones, as a consequence of inducing adipogenesis, also increase mitochondrial expression in mature adipocytes (8). This major increase in mitochondrial content as adipocytes mature supports an important role for mitochondria in adipocyte function. However, this role has not been well defined, O_2 consumption in adipocytes has been measured and basal O_2 consumption is similar to most other cells, increasing with differentiation (7) and decreasing with age (9,10) when expressed per milligram protein. On the other hand, despite the low rate of FA oxidation, mitochondrial dysfunction leads to TG accumulation (11) implying that FA oxidation is essential to a lean phenotype.

Here we show a persistent basal rate of adipocyte O_2 consumption despite the stimulation with the chemical uncoupler of oxidative phosphorylation, carbonylcyanide p-trifluoromethoxyphenylhydrazone (FCCP). We demonstrated that stimulation of uncoupled O_2 consumption required scavenging reactive oxygen species (ROS) by pyruvate or N-acetylcysteine (NAC). These data suggested that ROS-inhibited O_2 consumption may explain the difficulty in identifying effective strategies to increase fat burning and subsequent fat loss in adipocytes.

METHODS AND PROCEDURES

In vivo studies

C57BL/6J mice were fed a high-fat diet (35% fat-derived energy from Harlan Teklad-TD. 94059). NAC was added to drinking water (3 mg/ ml) and replaced daily except Saturday and Sunday. On day 1 and day 10 after the start of treatment, whole body fat mass and lean mass were measured *in vivo* without anesthesia, using EchoMRI-700/100 whole body composition analyzer (Echo Medical Systems, Houston, TX). Total body weight was measured by direct weighing. Percentage of fat mass was calculated as the ratio between fat

mass and total body weight multiplied by 100. Between day 12 and day 15, each mouse was placed in a single metabolic cage of the VO_2/VCO_2 OxyMax system (Columbus Instrument, Columbus, OH), with free access to drinking water. Food was provided *ad libitum* for the first 24 h and removed for the next 24 h. Measuring the changes of O_2 and CO_2 between input and output air continuously monitored respiration. Data acquired during the first 2 h of each experimental setup were discarded to minimize random fluctuation due to manual disturbance. The mean O_2 consumption and CO_2 generation rates were averaged separately in the dark period (19:00–7:00 h) and light period (7:00–19:00 h), each under fed and fasting conditions.

Isolation of adipocytes

White adipocytes were isolated from male Sprague–Dawley rat (230–260 g, Charles River Laboratories, Wilmington, MA) epididymal and perirenal fat depots by collagenase digestion, as described previously (3,12). Briefly, fat pads from the perirenal and epididymal depots were removed, and transferred into Krebs-Ringer Phosphate HEPES (KRP) buffer (containing 2% bovine serum albumin (BSA), 130 mmol/l NaCl, 4.7 mmol/l KCl, 1.24 mmol/l $MgSO_4$, 2.5 mmol/l $CaCl_2$, 10 mmol/l HEPES, 2.5 mmol/l NaH_2PO_4, 5 mmol/l D-glucose, and 200 nmol/l adenosine, pH 7.4) at 37 °C. Adipose tissue pieces were minced, and digested with collagenase B (1 mg/ml) in KRP buffer for 35 min at 37 °C in a shaking water bath. The fat cell suspension thus obtained was filtered through a 250 μm nylon mesh, and centrifuged for 15 s at 1,000 rpm. The adipocytes collected from the top phase were washed with KRP buffer three times. The cells were resuspended in three volumes of KRP buffer, allowed to equilibrate for 15 min at 37 °C, and then used directly for the subsequent experiments. The Institutional Animal Care and Use Committee of Boston University School of Medicine approved the animal use protocol.

O_2 consumption *in vitro*

O_2 consumption was measured as described previously (13–15). Reactions were carried out in KRP buffer for adipocyte O_2 consumption or in standard reaction medium (containing 1% BSA, 250 mmol/l sucrose, 10 mmol/l KCl, 5 mmol/l KH_2PO_4, 20 mmol/l HEPES, 2.5 mmol/l $MgCl_2$, 0.2 mmol/l EDTA (K^+ salt), pH 7.2) for mitochondrial O_2 consumption. O_2 consumption was measured at 37 °C for adipocytes or at 25 °C for mitochondria using a Clark-type O_2-sensitive electrode with amplifier in a stirred, water-jacketed, closed, silicon-coated chamber as described previously (13). Correction was made for electrode drift. The low rate of O_2 consumption, observed in the presence of the medium alone and due to O_2 use by the electrode, was subtracted from the subsequent rates. Further increases in O_2 consumption were observed upon sequential addition of cells or mitochondria. After recording the basal O_2 consumption (cell or mitochondria), fuel substrates and other chemicals (FCCP, rotenone, and NAC) were added by injection through an injection port while continuously monitoring O_2 consumption. Results were converted into nmol of O_2 used based on the dissolved O_2 in the medium of 225 μmol/l. O_2 consumption by adipocytes was expressed per milligram cell protein for ease of comparison with other cell types. Absolute O_2 consumption rates are expressed per milligram cell protein for ease of comparison with other cell types. In our preparations 1 mg adipocyte protein was equivalent to 2.6×10^6 cells or 16 μg DNA.

Measurement of glucose and endogenous FA conversion to CO_2

Glucose and endogenous FA oxidation were determined by collecting CO_2 released from glucose or FA oxidation. Adipocytes were incubated with [U-^{14}C] glucose for glucose oxidation studies or prelabeled with [U-^{14}C] palmitate for endogenous FA oxidation. The $^{14}CO_2$ released from endogenous palmitate in adipocytes was determined as previously described (3,14). Briefly, isolated adipocytes were prelabeled with 1 μCi/ml [U-^{14}C] palmitate in KRP buffer (2% BSA) for 30 min at 37 °C with gentle shaking. The cells were washed with KRP buffer three times to remove labeled palmitate from the medium. Glucose conversion to CO_2 was done in the same media except that [U-^{14}C] glucose (0.027 μCi/ml) was present during the final incubation. The incubation was carried out in 25-cm^2 culture flasks sealed with a rubber stopper from which a plastic well was suspended. Four milliliters of adipocyte suspension (1 ml of packed cell volume) either prelabeled with [U-^{14}C] palmitate or containing [U-^{14}C] glucose were incubated in the sealed flask for 2 h at 37 °C with gentle shaking. A folded filter paper (1 cm^2) was placed inside the well. At the end of the incubation period, the $^{14}CO_2$ produced by the adipocytes was released from the media by injection of 0.5 ml of 10 N H_2SO_4 into the flask. β-Phenethylamine (0.3 ml) was injected into the center well to absorb $^{14}CO_2$. After overnight equilibration at room temperature, each center well with filter paper containing the absorbed $^{14}CO_2$ was transferred into a 20-ml scintillation vial with 5 ml of scintillation fluid for β-counting. Counts from cell-free media were used as a blank. Calculations of endogenous FA oxidation were based on the specific activity of the prelabeled lipid pool. Calculations of glucose oxidation were based on the specific activity of glucose in the incubation media.

Adipocyte immobilization

The Matrigel method of Lynch *et al.* (16–18) was used to allow culturing and microscopy of primary adipocytes for several days. These cells maintained their normal spherical configuration and possessed a single large lipid droplet. Buffer was removed from fat cells and cells were washed twice and collected in a 15 ml tube. Tissue culture media (Dulbecco's modified Eagle medium from Gibco (Grand Island, NY) with 10% fetal bovine serum) was added to cells. Cells were allowed to rest at 37 °C for 30 min. In the modified method, 2% LMP Agarose (cat. no. 15517-022; Invitrogen, Carlsbad, CA) was prepared with phosphate buffered saline (Gibco cat. no. 14190-144) and maintained at 37–40 °C to prevent solidification. Cells (300 μl) were transferred to a 1.5 ml tube and mixed gently and thoroughly with 100 μl gel at 37 °C. A drop of the mixture was placed in the middle of a culture plate (part no. P35GC-0-10-C; MatTek, Ashland, MA), turned up side down, to allow fat cells to rise to the bottom of the plate, and maintained at room temperature for 5 min to allow gel formation. Then dishes were turned right side up and culture medium was added and cells maintained in a 37 °C incubator equilibrated with 5% CO_2.

Confocal microscopy

Mitochondria were labelled using the mitochondria-specific dyes. MitoTracker Green and tetramethylrhodamine ethyl ester perchlorate (TMRE, 7 nmol/l) were from Molecular Probes, (Eugene, OR). Freshly prepared TMRE was added to culture in ethanol from a 1,000,000 × stock to give a final concentration of 7 nmol/l and incubated for 1 h prior to

visualization. Confocal microscopy was performed on live cells using a Leica Confocal microscope (TCS SP2) with the following lasers Kr (568/20 mW), and Ar (488/20 mW).

Mitochondrial membrane potential ($\Delta\Psi_M$)

To image $\Delta\Psi_M$ in fat cells labelled with TMRE, cells were excited with a 568-nm laser, and emission was recorded through a BP 650–710-nm filter. *Z* sections of 1,024 × 1,024 images were obtained using a ×100 immersion oil lens. In this way both perinuclear and peripheral mitochondria were imaged. Metamorph image analysis software was used for image processing and analysis. As described by O'Reilly *et al.* (19), the $\Delta\Psi_M$-dependent component of TMRE accumulates in a Nernstian fashion that can be described by the intensity of its fluorescence. The non-$\Delta\Psi_M$-dependent component of TMRE, also known as the binding component, was ignored as it is fixed and voltage-independent. For microplate assay, cells were incubated with 20 nmol/l TMRE in the loading buffer (containing 140 mmol/l NaCl, 6 mmol/l KCl, 1 mmol/l $MgCl_2$, 5 mmol/l HEPES, 1.8 mmol/l $CaCl_2$, 5.8 mmol/l D-glucose, pH 7.4) for 30 min at 37 °C. Then cells were washed three times and incubated with KRP buffer (1% BSA). Basal fluorescent intensity (Ex.549/Em.574) was measured by a temperature-controlled microplate reader (Safire2; Tecan US, Durham, NC) at 37 °C. Next, cells were treated with FCCP (30 μmol/l), NAC (10 mmol/l), palmitate (0.4 mmol/l) or buffer, and the kinetic fluorescent intensities were recorded immediately for 10 min. For data analysis, the fluorescent intensities after chemical addition were first normalized to their respective basal values, then comparing with the appropriate control group at same time point. Final results were calculated by averaging the ratios between treated and control group at all time points.

ATP/ADP assay

Cells were extracted in cold 1% (wt/vol) trichloroacetic acid. Fat was removed by washing with two volumes of chloroform. Trichloroacetic acid was removed from the aqueous layer with four equal volume washes of diethyl ether using vacuum suction to completely remove the ether between each wash. Neutralized supernatants were then freeze-dried in a SpeedVac (Savant, Thermo Scientific, Waltham, MA) and stored at −80 °C until assayed. Dried samples were redissolved in water and an aliquot removed to measure adenosine triphosphate (ATP) directly with luciferase using a Turner Model 20e luminometer equipped with a Cavro injector. Adenosine diphosphate (ADP) was converted to ATP to be assayed by luciferase, after the sample was depleted of endogenous ATP with ATP sulphurylase (20). Data are presented as the ATP/ADP ratio, making them independent of changes in cell number per well or loss of sample volume during extraction (20).

Adipocyte and liver mitochondria

Mitochondria from adipocytes and liver were prepared according to standard procedures (21) and as described previously (4,22) with a slight modification. Adipocytes prepared from epididymal and perirenal fat pads or minced liver were suspended in two volumes of ice-cold homogenization buffer (containing 0.25 mol/l sucrose, 20 mmol/l HEPES, 0.2 mmol/l EDTA (K^+ salt) pH 7.4), and homogenized in a loose fitting homogenizer. Homogenates were centrifuged at 600 *g* for 10 min at 4 °C. The supernatant was centrifuged at 10,000 *g* for 10 min at 4 °C. The pellets containing mitochondria were suspended in 10 volumes of

0.25 mol/l sucrose and centrifuged at 10,000 *g* for 10 min at 4 °C. The mitochondrial pellet obtained was resuspended in homogenization buffer to give a final concentration of 1–3 mg of mitochondrial protein/ml, and stored on ice. Protein concentration of adipocyte and liver mitochondria was determined with the Bradford reagent using BSA as a standard.

ROS measurement

Intracellular ROS levels were measured using the 5-(and-6)-chloromethyl-2′, 7′-dichlorodihydrofluorescein diacetate, acetyl ester (CM-H_2DCF-DA, Molecular Probes), a cell permeable nonfluorescent precursor. This dye measures H_2O_2, ROO^-, and $ONOO^-$. Within the cells, CM-H_2DCFH-DA is hydrolyzed by nonspecific esterases to release CM-H_2DCF, which is readily oxidized by intracellular ROS. The oxidized product emits green fluorescence (Ex.475/Em.515). The protocol was modified from manufacture's instruction. Briefly, cells were loaded with 0.5 μmol/l CM-H_2DCF-DA for 20 min at 37 °C in the same loading buffer used in TMRE microplate assays. Then cells were washed three times and incubated with KRP buffer (1% BSA) for 1 h at 37 °C, with or without NAC (10 or 20 mmol/l), pyruvate (5 mmol/l), or H_2O_2 (1 mmol/l). The fluorescence intensity was measured by a microplate reader.

Materials

Collagenase B was from Boehringer Mannhein (Mannhein, Germany), LMP from Invitrogen, TMRE, CM-H_2DCF-DA from Molecular Probes, Luciferase from Becton Dickinson (Bedford, MA), BSA FA-free from American Bioanalytical (Natick, MA), media and sera from Gibco, dishes from MatTek. Glass bottom culture dishes were from MatTek. Matrigel Matrix was from Becton Dickinson. Other chemicals were from Sigma Chemical (St Louis, MO). [U-^{14}C] glucose and [U-^{14}C] palmitate were from NEN (Boston, MA).

Statistical analysis

Microcal Origin 50 (Microcal Software, Northampton, MA) was used for statistical analysis. Values are shown in figures and tables as means of the number of separate measurements (*n*) ± s.e. Comparisons were performed using ANOVA. $P < 0.05$ was considered significant.

RESULTS

Influence of fuels on adipocyte O_2 consumption

Cellular O_2 consumption is mainly a reflection of mitochondrial respiration from glucose and FA to generate a constant level of ATP and maintain a highly negative mitochondrial membrane potential to drive ATP production. To study control of adipocyte respiration, fuel-stimulated O_2 consumption in intact cells was evaluated. Table 1 shows that basal (5 mmol/l glucose) adipocyte O_2 consumption (4.3 ±0.18 nmol/min/mg protein, $n = 65$) is within the range of values reported for other cell types (23–25) when expressed per milligram protein. Basal O_2 consumption is normally about 25–30% of maximal O_2 consumption. However, unlike other cells, FCCP addition did not increase O_2 consumption in adipocytes (Table 1, top row, FCCP column). The possibility that insufficient substrate supply could account for the failure to increase uncoupled O_2 consumption appeared to be unlikely because addition of a wide variety of substrates including acetate, octanoate, methyl-succinate, malate,

glutamine, lactate, and combinations thereof caused only small but insignificant changes in O_2 consumption (Table 1).

Interaction of FA and oxidative metabolism

The possibility that the high-fat environment of adipocytes might inhibit fuel oxidation was considered because the metabolically active intracellular FA product, LC-CoA, has been reported to inhibit O_2 consumption and substrate transport into the mitochondria (26–28). However, exogenous FA did not inhibit either glucose or endogenous FA oxidation in adipocytes but rather exerted a stimulatory effect on glucose oxidation at high FA concentrations (Supplementary Figure S1a online). Consistent with the lack of effect of FA on endogenous FA oxidation (Supplementary Figure S1b online), exogenous FA did not significantly stimulate O_2 consumption either (2.66 ± 0.26 and 3.42 ± 0.37 nmol/min/mg, control vs. 0.5 mmol/l palmitate, $n = 9$). We previously documented little effect of glucose on FA oxidation (4). Thus, although FA oxidation is very low in adipocytes, FA do not appear to inhibit either glucose or FA oxidation under the conditions tested.

The pyruvate effect

In contrast to the lack of FCCP stimulation of respiration by other fuels and fuel combinations, pyruvate stimulated more than a threefold increase in O_2 consumption in uncoupled adipocytes (Table 1, bottom row, and Figure 1a). Stimulation of uncoupled O_2 consumption by pyruvate was concentration-dependent with a half-maximal effect at ~0.3 mmol/l (Figure 1a). Stimulated O_2 consumption was also dependent on the concentration of FCCP with a rather high maximal effect at about 20 μmol/l (Figure 1b). This high concentration of FCCP may be due to its lipophilicity and distribution into the fat droplet. Pyruvate is metabolized in the cytosol where it can be converted to lactate via lactate dehydrogenase and in the mitochondria where it serves as a source of acetyl CoA for the citric acid cycle.

To determine whether pyruvate action occurred in mitochondria or cytosol, we tested the ability of the mitochondrial pyruvate transport inhibitor α-cyanocinnamic acid (Cyncin) (29), to modulate pyruvate stimulation of FCCP-induced O_2 consumption. Figure 1c shows that Cyncin inhibited basal O_2 consumption suggesting that a major component of basal respiration required pyruvate transport into the mitochondria. Cyncin also markedly abrogated the stimulatory effect of pyruvate plus FCCP on O_2 consumption to levels below basal. In order to rule out the possibility that Cyncin nonspecifically inhibited the plasma membrane pyruvate carrier, we evaluated methyl-pyruvate (MePyr), which is a carrier-independent cell permeant ester that is converted to pyruvate in the cytosol following methyl ester cleavage by esterases. As shown in Figure 1c, MePyr was nearly as effective as pyruvate in stimulating O_2 consumption with FCCP and this effect was totally blocked by Cyncin. These data indicate that pyruvate must enter the mitochondria to exert its stimulatory effect, implicating an intramitochondrial site of inhibited O_2 consumption.

Sensitivity of adipocyte mitochondria to uncoupling

Chemical uncouplers like FCCP act as proton ionophores to collapse the mitochondrial membrane potential. This causes a decrease in the ATP/ADP ratio due to loss of the proton

motive force needed to synthesize ATP. To determine whether adipocyte mitochondria were initially coupled and became uncoupled in response to FCCP, we measured mitochondrial membrane potential ($\Delta\Psi_M$ and the cellular ATP/ADP ratio. For $\Delta\Psi_M$ assessments, adipocytes were immobilized upside down in a gel. Mitochondrial localization was determined using the mitochondria-specific dye, MitoTracker green. Figure 2a (left) shows a three dimensional reconstruction of an immobilized spherical adipocyte with a high concentration of mitochondria in the vicinity of the nucleus. Figure 2a also illustrates a single plane through an immobilized adipocyte before (middle) and after (right) FCCP addition. Comparing the intensity of the TMRE images as well as the merged images, it is clear that FCCP addition decreased $\Delta\Psi_M$. This result was also confirmed using a microplate assay (Figure 2b). NAC is a powerful antioxidant that also increases cellular glutathione content, thus facilitating removal of H_2O_2 by glutathione peroxidase (30). We found that NAC decreased $\Delta\Psi_M$. Palmitate also decreased $\Delta\Psi_M$ though less extensively.

To determine whether the decreased $\Delta\Psi_M$ had the expected effect of lowering the ATP/ADP ratio, adipocytes were incubated with and without FCCP for 10 min and the ratio determined in deproteinized cell extracts. Figure 2c shows that the basal ATP/ADP ratio was high (12.1 ±1.4) as expected with well-coupled adipocyte mitochondria. There was little effect of pyruvate addition on the ratio, consistent with an adequate endogenous supply of mitochondrial substrate. As expected, FCCP reduced the ATP/ADP ratio to <1 (Figure 2c).

Taken together, the data from Figures 2a–c indicate that FCCP effectively uncoupled previously well-coupled adipocyte mitochondria, a maneuver that generally elicits maximum O_2 consumption as cells strive to restore the mitochondrial membrane potential and ATP/ADP ratio using any available fuel. However, uncoupling did not stimulate O_2 consumption in adipocytes in the absence of pyruvate as illustrated in Table 1 and Figure 1c.

Isolated adipocyte mitochondria

To determine whether adipocyte mitochondria were unusual in their fuel preferences and possibly preferred pyruvate as substrate due to expression of the mitochondrial pyruvate carrier preferentially over other anion carriers, the fuel preferences of mitochondria isolated from adipocyte and liver were compared. Table 2 shows that the isolated mitochondria from both liver and adipocytes were well coupled. The data also indicate that succinate elicited the greatest rate of O_2 consumption in adipocyte mitochondria as has been shown in mitochondria from other cell types (31) and, although pyruvate was an excellent fuel, succinate was better. Thus, an unusual preference for pyruvate or transport of pyruvate could not explain the unique ability of this substrate and not succinate to enhance uncoupled O_2 consumption in adipocytes. This unique preference for pyruvate suggested that pyruvate stimulation of uncoupled O_2 consumption was not a consequence of its fuel function.

Adipocyte ROS

In addition to its well-established roles as a fuel, oxidant in the cytosol (via lactate dehydrogenase) and reducing agent in the mitochondria (via pyruvate dehydrogenase), pyruvate has long been known to act as a chemical scavenger of ROS (32,33). We tested the possibility that it was ROS scavenging that explained pyruvate's ability to stimulate

uncoupled O_2 consumption. First, we found that cells exposed to NAC exhibited a stimulation of O_2 consumption even greater than pyruvate, supporting the concept that ROS plays a role in the inhibition of O_2 consumption (Figure 1d). Interestingly, NAC tended to decrease both $\Delta\Psi_M$ (Figure 2b) and the ATP/ADP ratio (Figure 2c), which may have contributed to its ability to stimulate respiration. However, these changes were not statistically significant.

Second, we assessed ROS levels directly in isolated adipocytes using CM-H_2DCF-DA. Figure 2d illustrates that the presence of pyruvate, FCCP or both significantly decreased ROS by 15–30% whereas NAC decreased ROS by 40% in adipocytes, as reported previously by others (30,34,35). The addition of H_2O_2, as a positive control, caused a large increase in fluorescence. These data are consistent with the well-established role of pyruvate and NAC as ROS scavengers.

Third, we examined whether the role of pyruvate as ROS scavenger and energy substrate could be distinguished in FCCP-treated fat cells. Rotenone is a chemical inhibitor of mitochondrial complex I. At a concentration of 1 μmol/l and above, rotenone completely inhibited FCCP-stimulated respiration in the presence of pyruvate (Figure 3a). However, further addition of methyl-succinate, a substrate of mitochondrial complex II that bypasses the rotenone block in the respiratory chain, significantly increased respiration by 129% over basal (Figure 3b, black bars). On the other hand, methyl-succinate only increased respiration by 34% in the absence of pyruvate (Figure 3b, gray bars). Thus, in the presence of FCCP to uncouple, and pyruvate to scavenge ROS, methyl-succinate stimulated respiration although it was unable to do this alone (Table 1).

In vivo ROS scavenging

Previous studies indicated that NAC increases O_2 consumption in rats (36) and reduces visceral fat in mice (37). To assess the possible relevance of ROS scavenging on fat mass *in vivo*, mice were given NAC in their drinking water. After 10 days of high-fat feeding, compared to Day 1, there was significantly less gain in body fat as assessed by NMR (Figure 4a) with no difference in body weight gain in mice given NAC. After 12–15 days on the diet, the both fed and 18 h fasted mice given NAC had significantly higher O_2 consumption and CO_2 production than the controls (Figure 4b). These differences were most pronounced during the light cycle or inactive period implying an increase in resting energy expenditure.

DISCUSSION

The surprising finding from these studies is that O_2 consumption above basal is inhibited in adipocytes but can be stimulated by removing ROS. This implies either high sensitivity of adipocyte O_2 consumption to normal levels of ROS or high levels of ROS in adipocytes. The latter explanation is more likely because many studies have documented that increased adiposity is accompanied by increased oxidative stress and infiltration of adipose tissue with macrophages. This suggests that inhibition of O_2 consumption and high levels of ROS are tolerated and possibly serve an important function in adipocytes unlike other cell types where oxidative stress and ROS lead to apoptosis. Such unique tolerance could lead to a thrifty phenotype by limiting fat burning and promoting fat storage.

ROS and mitochondrial function

It is known that various reactive species inhibit O_2 consumption and stimulate apoptosis (38–40). Data from obese mice indicate ROS levels increase selectively in adipose tissue (35). Our data and other studies in the literature suggest that ROS levels are high in adipocytes (30,34), suggesting unusual tolerance. Mitochondrial function is also important for TG storage in adipocytes. It has been shown previously that mitochondrial dysfunction in adipocytes leads to increased TG storage (11) and that aging is accompanied by decreased mitochondrial function and increased lipid stores (41–43). Our findings suggest that limited mitochondrial O_2 consumption occurred spontaneously and may be one of the unique attributes of adipocytes.

Increased ROS or increased ROS sensitivity

Adipocytes isolated from mice fed a high-fat diet (35) or exposed to nutrient excess *in vivo* (30) display significantly elevated ROS *in vitro*. Thus, adipocytes appear to reside in a relatively high ROS environment due both to endogenous and exogenous ROS production from resident macrophages. Despite such a potentially damaging environment, adipocytes appear relatively insensitive to the damaging effects of ROS.

Differentiation of murine 3T3-L1 preadipocytes into adipocytes is associated with the acquisition of apoptotic resistance accompanied by upregulation of cell survival genes even under conditions where ROS production is increased (44). Interestingly, human cells appear to be protected from apoptosis through an autocrine/paracrine action of IGF-1, which maintains the expression of antiapoptotic proteins, Bcl- (XL) and Fas–associated-death-domain protein like IL-1-converting-enzyme-inhibitory protein (45). Thus, ROS and inflammation exist in adipocytes (30,34,35) and this appears to occur in response to the same stimuli that increase ROS in other cells but these do not lead to the expected increase in damage, presumably due to the protective effect of antiapoptotic proteins (45–47). The mechanistic basis for tolerance of high levels of ROS requires further investigation.

ROS scavenging and pyruvate

Pyruvate has several fates in the cell. It is converted to lactate in the cytosol with accompanying conversion of NADH to NAD. This cannot explain our findings because the data show that stimulation of O_2 consumption by FCCP in adipocytes requires intramitochondrial pyruvate. Pyruvate is also converted to acetyl CoA in the mitochondria with accompanying conversion of NAD to NADH. Although this is likely to occur, it also cannot explain our findings because other mitochondrial fuels also increase mitochondrial NADH but do not stimulate respiration (Table 1). In addition, we were still able to take advantage of the ability of pyruvate to scavenge ROS after inhibiting its metabolism with rotenone and using an alternative substrate, succinate (administrated as methyl-succinate), that bypassed the respiratory block. Our findings are consistent with other diverse findings reported in the literature. The ability of pharmacological levels of pyruvate to protect cells by nonenzymatic scavenging of ROS has been demonstrated in cardiac cells and neurons (32,33,48–49) in addition to our findings here. This is not surprising because most ROS is produced in the mitochondria.

The reason why NAC is more powerful than pyruvate (Figure 1c vs. 1d) may relate to its greater oxidative potential or to its ability to slightly decrease the $\Delta\Psi_M$ (Figure 2b) and ATP/ADP ratio (Figure 2c). Clearly the decrease in $\Delta\Psi_M$ was not sufficient, although it may be necessary, because FA also slightly depolarized the mitochondria but did not stimulate respiration. NAC may also increase glutathione within the mitochondria, which may be important if glutathione levels are low in adipocytes. Glutathione levels in adipocyte mitochondria have not been reported. Alternatively, glutathione generated by NAC may cause the mitochondrial redox state to be more oxidized (50,51) whereas pyruvate causes a more reduced state. It has been shown that a highly reduced state favors ROS generation. In addition, mitochondrial efflux of H_2O_2 may also exert additional effects in the cytosol. There may also be a component of the cytosolic glutathione redox state that contributes to respiratory inhibition.

Interestingly, the *in vivo* effect of NAC on respiration and body fat has also been reported in other studies. Novelli *et al.* demonstrated that in Wistar rats on a high-sucrose diet, 30-day NAC feeding increased O_2 consumption, decreased respiratory quotient without affecting total energy intake (36). In the other study by Kim *et al.*, injecting C57BL/6 mice with NAC for 8 weeks dose-dependently decreased visceral fat mass and body weight (37). Though the authors of the second study suggested that NAC inhibits preadipocyte differentiation, our conclusion on NAC-induced respiration could offer an alternative explanation.

Inhibition of O_2 consumption

The documentation of uncoupling in intact cells in the presence of adequate fuel and O_2 without an increase in O_2 consumption is unusual and has not been previously reported to our knowledge. In most cells decreased mitochondrial $\Delta\Psi_M$, chemical uncoupling of oxidative phosphorylation or a large fall in the ATP/ADP ratio, as we found (Figures 2b and c), stimulate O_2 consumption (26–28). Among other putative factors known to inhibit O_2 consumption, we ruled out FA-induced inhibition of fuel oxidation (Supplementary Figure S1 online), lack of fuel (Table 1), O_2 deprivation (through direct measurement) and high ATP levels in the presence of an uncoupler (Figure 2c). Although FA and glucose have been shown to compete for entry into the Krebs cycle in many cells, this does not occur to a significant extent in adipocytes (Supplementary Figure S1 online). Because LC-CoA levels are likely to be high in adipocytes in order to handle the high FA fluxes, another possibility is inhibition of the adenine nucleotide translocase or other mitochondrial anion carriers (52–57) by LC-CoA. None of these mechanisms appear to explain inhibition of uncoupled respiration in adipocytes since it can be overcome by ROS removal. Furthermore, administration of NAC to whole animals increases O_2 consumption and decreases body fat suggesting that ROS scavenging or provision of glutathione from NAC also stimulates respiration *in vivo*. It should be noted that others have attributed NAC effectiveness to alterations in β-hydroxyacyl CoA dehydrogenase (58) or metalothionine II (37). These correlations may be relevant, are not mutually exclusive but do not provide a mechanistic explanation for the observed increase in respiration.

The thrifty phenotype

The concept of a thrifty phenotype was introduced by Hales in 1992 to explain a high incidence of type 2 diabetes in individuals exposed to gestational malnourishment (59). The rationale for such a mechanism is to adapt the unborn child to survival under circumstance of inadequate nutrition; however, a molecular mechanism underpinning this phenomenon has not been elucidated. The data presented here suggest that genes that prevent fat burning and promote storage are among the attributes of normal fat cells. Thus, fat cells by virtue of their unique function exhibit a thrifty phenotype. The particular genes involved could include those that confer protection from cell damage. Deprivation, whether gestational or due to dieting, could induce these genes. It is well-established that the genetic profile of a reduced obese individual is different from a never-obese individual of the same weight (60,61). Thus, a thrifty phenotype is hypothesized to result from nutritional excess in individuals who are unable to overcome ROS inhibition of O_2 consumption in their fat cells. It will be interesting to determine whether there are variations in ROS sensitivity that correlate with obesity and leanness. A further implication of this hypothesis is that excess ROS in other cell types might also inhibit O_2 consumption and cause ectopic fat storage.

The model

A testable model that evolves from our data has four important constituents: (i) high levels of FA, as occur normally in fat cells, increase ROS production; (ii) a relatively sluggish scavenging system, particularly in mitochondria, allows elevated ROS levels to be maintained; (iii) ROS inhibits O_2 consumption; (iv) an enhanced adipocyte defense system tolerates levels of ROS sufficient to inhibit O_2 consumption without inducing cell damage. As a result, fat cannot be burned and TG storage is favored. It is predicted that preventing or reversing the four constituents described above will decrease TG stores and test the model. Testing this model is the focus of our current work.

Supplementary Material

Refer to Web version on PubMed Central for supplementary material.

Acknowledgments

This work was supported by NIH grants: DK56690, DK46200 (B.E.C.), DK74778 (O.S.), and DK59261 (W.G.).

References

1. McGarry JD, Takabayashi Y, Foster DW. The role of malonyl-coa in the coordination of fatty acid synthesis and oxidation in isolated rat hepatocytes. J Biol Chem. 1978; 253:8294–8300. [PubMed: 711753]
2. Wang YL, Guo W, Zang Y, et al. Acyl coenzyme a synthetase regulation: putative role in long-chain acyl coenzyme a partitioning. Obes Res. 2004; 12:1781–1788. [PubMed: 15601973]
3. Wang T, Zang Y, Ling W, Corkey BE, Guo W. Metabolic partitioning of endogenous fatty acid in adipocytes. Obes Res. 2003; 11:880–887. [PubMed: 12855758]
4. Zang Y, Wang T, Xie W, et al. Regulation of acetyl CoA carboxylase and carnitine palmitoyl transferase-1 in rat adipocytes. Obes Res. 2005; 13:1530–1539. [PubMed: 16222055]

5. Wilson-Fritch L, Burkart A, Bell G, et al. Mitochondrial biogenesis and remodeling during adipogenesis and in response to the insulin sensitizer rosiglitazone. Mol Cell Biol. 2003; 23:1085–1094. [PubMed: 12529412]
6. Wilson-Fritch L, Nicoloro S, Chouinard M, et al. Mitochondrial remodeling in adipose tissue associated with obesity and treatment with rosiglitazone. J Clin Invest. 2004; 114:1281–1289. [PubMed: 15520860]
7. von Heimburg D, Hemmrich K, Zachariah S, Staiger H, Pallua N. Oxygen consumption in undifferentiated versus differentiated adipogenic mesenchymal precursor cells. Respir Physiol Neurobiol. 2005; 146:107–116. [PubMed: 15766899]
8. Bogacka I, Xie H, Bray GA, Smith SR. Pioglitazone induces mitochondrial biogenesis in human subcutaneous adipose tissue *in vivo*. Diabetes. 2005; 54:1392–1399. [PubMed: 15855325]
9. Kim JH, Woldgiorgis G, Elson CE, Shrago E. Age-related changes in respiration coupled to phosphorylation. I. Hepatic mitochondria. Mech Ageing Dev. 1988; 46:263–277. [PubMed: 2852281]
10. Wallace DC. Mitochondrial diseases in man and mouse. Science. 1999; 283:1482–1488. [PubMed: 10066162]
11. Vankoningsloo S, Piens M, Lecocq C, et al. Mitochondrial dysfunction induces triglyceride accumulation in 3T3-L1 cells: role of fatty acid beta-oxidation and glucose. J Lipid Res. 2005; 46:1133–1149. [PubMed: 15741651]
12. Rodbell M. Metabolism of isolated fat cells. I. Effects of hormones on glucose metabolism and lipolysis. J Biol Chem. 1964; 239:375–380. [PubMed: 14169133]
13. Civelek VN, Deeney JT, Fusonie GE, Corkey BE, Tornheim K. Oscillations in oxygen consumption by permeabilized clonal pancreatic beta-cells (HIT) incubated in an oscillatory glycolyzing muscle extract: roles of free Ca2+, substrates, and the ATP/ADP ratio. Diabetes. 1997; 46:51–56. [PubMed: 8971081]
14. Civelek VN, Deeney JT, Shalosky NJ, et al. Regulation of pancreatic beta-cell mitochondrial metabolism: influence of Ca2+, substrate and ADP. Biochem J. 1996; 318(Pt 2):615–621. [PubMed: 8809055]
15. Saggerson ED. Utilisation of exogenous fatty acids by rat epididymal fat cells *in vitro*. Biochim Biophys Acta. 1976; 431:371–377. [PubMed: 949481]
16. Fox HL, Kimball SR, Jefferson LS, Lynch CJ. Amino acids stimulate phosphorylation of p70S6k and organization of rat adipocytes into multicellular clusters. Am J Physiol. 1998; 274:C206–C213. [PubMed: 9458729]
17. Brown LM, Fox HL, Hazen SA, et al. Role of the matrixin MMP-2 in multicellular organization of adipocytes cultured in basement membrane components. Am J Physiol. 1997; 272:C937–C949. [PubMed: 9124530]
18. Hazen SA, Rowe WA, Lynch CJ. Monolayer cell culture of freshly isolated adipocytes using extracellular basement membrane components. J Lipid Res. 1995; 36:868–875. [PubMed: 7616129]
19. O'Reilly CM, Fogarty KE, Drummond RM, Tuft RA, Walsh JV Jr. Quantitative analysis of spontaneous mitochondrial depolarizations. Biophys J. 2003; 85:3350–3357. [PubMed: 14581236]
20. Deeney JT, Köhler M, Kubik K, et al. Glucose-induced metabolic oscillations parallel those of Ca(2+) and insulin release in clonal insulin-secreting cells. A multiwell approach to oscillatory cell behavior. J Biol Chem. 2001; 276:36946–36950. [PubMed: 11481328]
21. Johnson D, Lardy H. Isolation of liver or kidney mitochondria. Methods Enzymol. 1967; 10:94–96.
22. Kotlyar AB, Maklashina E, Cecchini G. Absence of NADH channeling in coupled reaction of mitochondrial malate dehydrogenase and complex I in alamethicin-permeabilized rat liver mitochondria. Biochem Biophys Res Commun. 2004; 318:987–991. [PubMed: 15147970]
23. Curti D, Rognoni F, Gasparini L, et al. Oxidative metabolism in cultured fibroblasts derived from sporadic Alzheimer's disease (AD) patients. Neurosci Lett. 1997; 236:13–16. [PubMed: 9404940]
24. Else PL, Brand MD, Turner N, Hulbert AJ. Respiration rate of hepatocytes varies with body mass in birds. J Exp Biol. 2004; 207:2305–2311. [PubMed: 15159435]
25. Qu W, Zhong Z, Arteel GE, Thurman RG. Stimulation of oxygen uptake by prostaglandin E2 is oxygen dependent in perfused rat liver. Am J Physiol. 1998; 275:G542–G549. [PubMed: 9724267]

26. Ferguson M, Mockett RJ, Shen Y, Orr WC, Sohal RS. Age-associated decline in mitochondrial respiration and electron transport in Drosophila melanogaster. Biochem J. 2005; 390:501–511. [PubMed: 15853766]
27. Rasmussen UF, Rasmussen HN. Human quadriceps muscle mitochondria: a functional characterization. Mol Cell Biochem. 2000; 208:37–44. [PubMed: 10939626]
28. Ventura FV, Ruiter J, Ijlst L, de Almeida IT, Wanders RJ. Differential inhibitory effect of long-chain acyl-CoA esters on succinate and glutamate transport into rat liver mitochondria and its possible implications for long-chain fatty acid oxidation defects. Mol Genet Metab. 2005; 86:344–352. [PubMed: 16176879]
29. Halestrap AP, Denton RM. The specificity and metabolic implications of the inhibition of pyruvate transport in isolated mitochondria and intact tissue preparations by alpha-Cyano-4-hydroxycinnamate and related compounds. Biochem J. 1975; 148:97–106. [PubMed: 1171687]
30. Lin Y, Berg AH, Iyengar P, et al. The hyperglycemia-induced inflammatory response in adipocytes: the role of reactive oxygen species. J Biol Chem. 2005; 280:4617–4626. [PubMed: 15536073]
31. Deveaud C, Beauvoit B, Salin B, Schaeffer J, Rigoulet M. Regional differences in oxidative capacity of rat white adipose tissue are linked to the mitochondrial content of mature adipocytes. Mol Cell Biochem. 2004; 267:157–166. [PubMed: 15663197]
32. Giandomenico AR, Cerniglia GE, Biaglow JE, Stevens CW, Koch CJ. The importance of sodium pyruvate in assessing damage produced by hydrogen peroxide. Free Radic Biol Med. 1997; 23:426–434. [PubMed: 9214579]
33. Mallet RT, Sun J. Antioxidant properties of myocardial fuels. Mol Cell Biochem. 2003; 253:103–111. [PubMed: 14619960]
34. Furukawa S, Fujita T, Shimabukuro M, et al. Increased oxidative stress in obesity and its impact on metabolic syndrome. J Clin Invest. 2004; 114:1752–1761. [PubMed: 15599400]
35. Talior I, Tennenbaum T, Kuroki T, Eldar-Finkelman H. PKC-delta-dependent activation of oxidative stress in adipocytes of obese and insulin-resistant mice: role for NADPH oxidase. Am J Physiol Endocrinol Metab. 2005; 288:E405–E411. [PubMed: 15507533]
36. Novelli EL, Santos PP, Assalin HB, et al. N-acetylcysteine in high-sucrose diet-induced obesity: energy expenditure and metabolic shifting for cardiac health. Pharmacol Res. 2009; 59:74–79. [PubMed: 18996201]
37. Kim JR, Ryu HH, Chung HJ, et al. Association of anti-obesity activity of N-acetylcysteine with metallothionein-II down-regulation. Exp Mol Med. 2006; 38:162–172. [PubMed: 16672770]
38. Giulivi C. Characterization and function of mitochondrial nitric-oxide synthase. Free Radic Biol Med. 2003; 34:397–408. [PubMed: 12566065]
39. Sadek HA, Szweda PA, Szweda LI. Modulation of mitochondrial complex I activity by reversible Ca2+ and NADH mediated superoxide anion dependent inhibition. Biochemistry. 2004; 43:8494–8502. [PubMed: 15222760]
40. Kagan VE, Borisenko GG, Tyurina YY, et al. Oxidative lipidomics of apoptosis: redox catalytic interactions of cytochrome c with cardiolipin and phosphatidylserine. Free Radic Biol Med. 2004; 37:1963–1985. [PubMed: 15544916]
41. Kirkland JL, Tchkonia T, Pirtskhalava T, Han J, Karagiannides I. Adipogenesis and aging: does aging make fat go MAD? Exp Gerontol. 2002; 37:757–767. [PubMed: 12175476]
42. Karagiannides I, Tchkonia T, Dobson DE, et al. Altered expression of C/EBP family members results in decreased adipogenesis with aging. Am J Physiol Regul Integr Comp Physiol. 2001; 280:R1772–R1780. [PubMed: 11353682]
43. Kirkland JL, Hollenberg CH, Kindler S, Gillon WS. Effects of age and anatomic site on preadipocyte number in rat fat depots. J Gerontol. 1994; 49:B31–B35. [PubMed: 8282974]
44. Carrière A, Fernandez Y, Rigoulet M, Pénicaud L, Casteilla L. Inhibition of preadipocyte proliferation by mitochondrial reactive oxygen species. FEBS Lett. 2003; 550:163–167. [PubMed: 12935904]
45. Fischer-Posovszky P, Tornqvist H, Debatin KM, Wabitsch M. Inhibition of death-receptor mediated apoptosis in human adipocytes by the insulin-like growth factor I (IGF-I)/IGF-I receptor autocrine circuit. Endocrinology. 2004; 145:1849–1859. [PubMed: 14691011]

46. Papineau D, Gagnon A, Sorisky A. Apoptosis of human abdominal preadipocytes before and after differentiation into adipocytes in culture. Metab Clin Exp. 2003; 52:987–992. [PubMed: 12898462]
47. Tchkonia T, Tchoukalova YD, Giorgadze N, et al. Abundance of two human preadipocyte subtypes with distinct capacities for replication, adipogenesis, and apoptosis varies among fat depots. Am J Physiol Endocrinol Metab. 2005; 288:E267–E277. [PubMed: 15383371]
48. Yanagida S, Luo CS, Doyle M, Pohost GM, Pike MM. Nuclear magnetic resonance studies of cationic and energetic alterations with oxidant stress in the perfused heart. Modulation with pyruvate and lactate. Circ Res. 1995; 77:773–783. [PubMed: 7554125]
49. Salahudeen AK, Clark EC, Nath KA. Hydrogen peroxide-induced renal injury. A protective role for pyruvate *in vitro* and *in vivo*. J Clin Invest. 1991; 88:1886–1893. [PubMed: 1752950]
50. Tukov FF, Rimoldi JM, Matthews JC. Characterization of the role of glutathione in repin-induced mitochondrial dysfunction, oxidative stress and dopaminergic neurotoxicity in rat pheochromocytoma (PC12) cells. Neurotoxicology. 2004; 25:989–999. [PubMed: 15474617]
51. Ushmorov A, Hack V, Dröge W. Differential reconstitution of mitochondrial respiratory chain activity and plasma redox state by cysteine and ornithine in a model of cancer cachexia. Cancer Res. 1999; 59:3527–3534. [PubMed: 10416620]
52. Shug A, Lerner E, Elson C, Shrago E. The inhibition of adenine nucleotide translocase activity by oleoyl CoA and its reversal in rat liver mitochondria. Biochem Biophys Res Commun. 1971; 43:557–563. [PubMed: 5563306]
53. Shug AL, Shrago E, Bittar N, Folts JD, Koke JR. Acyl-CoA inhibition of adenine nucleotide translocation in ischemic myocardium. Am J Physiol. 1975; 228:689–692. [PubMed: 1115232]
54. Woldegiorgis G, Shrago E, Gipp J, Yatvin M. Fatty acyl coenzyme A-sensitive adenine nucleotide transport in a reconstituted liposome system. J Biol Chem. 1981; 256:12297–12300. [PubMed: 6271781]
55. Woldegiorgis G, Yousufzai SY, Shrago E. Studies on the interaction of palmitoyl coenzyme A with the adenine nucleotide translocase. J Biol Chem. 1982; 257:14783–14787. [PubMed: 6294078]
56. Shrago E, Woldegiorgis G, Ruoho AE, DiRusso CC. Fatty acyl CoA esters as regulators of cell metabolism. Prostaglandins Leukot Essent Fatty Acids. 1995; 52:163–166. [PubMed: 7784453]
57. Woldegiorgis G, Lawrence J, Ruoho A, Duff T, Shrago E. Photoaffinity labeling of mitochondrial proteins with 2-azido [32P]palmitoyl CoA. FEBS Lett. 1995; 364:143–146. [PubMed: 7750558]
58. Diniz YS, Rocha KK, Souza GA, et al. Effects of N-acetylcysteine on sucrose-rich diet-induced hyperglycaemia, dyslipidemia and oxidative stress in rats. Eur J Pharmacol. 2006; 543:151–157. [PubMed: 16814277]
59. Hales HA, Peterson CM, Jones KP, Quinn JD. Leiomyomatosis peritonealis disseminata treated with a gonadotropin-releasing hormone agonist. A case report. Am J Obstet Gynecol. 1992; 167:515–516. [PubMed: 1497063]
60. Raben A, Mygind E, Astrup A. Lower activity of oxidative key enzymes and smaller fiber areas in skeletal muscle of postobese women. Am J Physiol. 1998; 275:E487–E494. [PubMed: 9725816]
61. Simoneau JA, Veerkamp JH, Turcotte LP, Kelley DE. Markers of capacity to utilize fatty acids in human skeletal muscle: relation to insulin resistance and obesity and effects of weight loss. FASEB J. 1999; 13:2051–2060. [PubMed: 10544188]

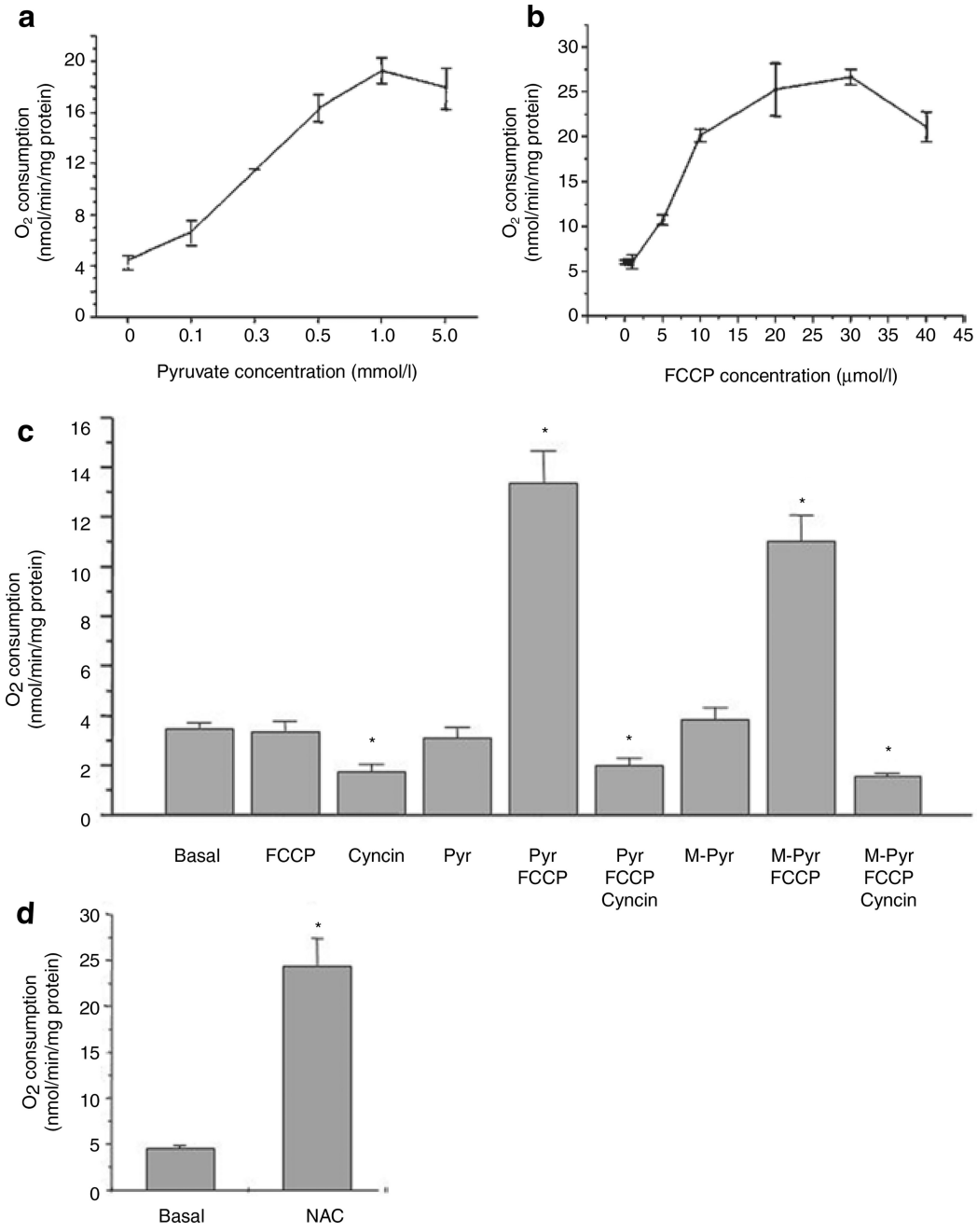

Figure 1.

O_2 consumption of isolated rat white adipocytes in the presence of different compounds. (**a**) Concentration dependence of pyruvate stimulated uncoupled O_2 consumption. O_2 consumption in intact adipocytes was measured at 37 °C in 1 ml of adipocyte suspension (adipocytes: KRP buffer 1:3, vol/vol), with 5 mmol/l glucose and 30 µmol/l carbonylcyanide p-trifluoromethoxyphenylhydrazone (FCCP) plus the indicated concentrations of pyruvate. Data are means ± s.e. of experiments from three separate preparations. (**b**) Concentration dependence of FCCP stimulated O_2 consumption. O_2 consumption in intact adipocytes was measured as described above with 5 mmol/l pyruvate plus the indicated concentrations of

FCCP. Data are means ± s.e. of experiments from three separate preparations. (**c**) The influence of different substrates and inhibitors on adipocyte O_2 consumption. O_2 consumption was measured under basal conditions or following addition of FCCP (30 μmol/l), Cyncin (5 mmol/l), pyruvate (5 mmol/l), MePyr (5 mmol/l) separately, or in combinations indicated. Data are means ± s.e., $n = 4$. (d) N-acetylcysteine (NAC) stimulated O_2 consumption. O_2 consumption was measured under basal conditions or following addition of 10 mmol/l NAC. Data are means ± s.e., $n = 4$. $^*P < 0.05$.

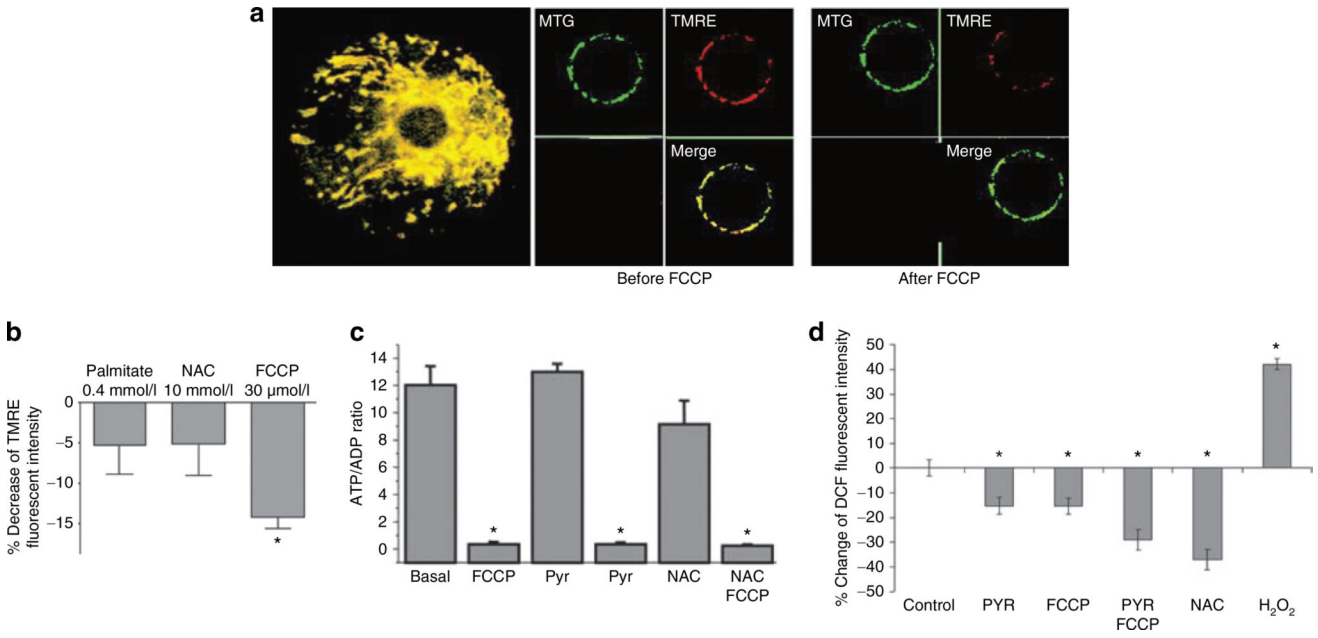

Figure 2.

Adipocyte mitochondrial membrane potential, adenosine triphosphate/adenosine diphosphate (ATP/ADP) ratio, and reactive oxygen species (ROS). (**a**) Left, three dimensional reconstruction of adipocyte mitochondria identified with MitoTracker Green (MTG). Single adipocytes exhibited a high concentration of mitochondria in the vicinity of the nucleus and sparse distribution of mitochondria around the equator. Middle and right, illustration of decreased mitochondrial membrane potential in adipocytes following carbonylcyanide p-trifluoromethoxyphenylhydrazone (FCCP) addition. A single plane through an immobilized adipocyte before (middle) and after (right) FCCP addition. Adipocytes were loaded with MTG to identify mitochondria (green image in upper left panels) and tetramethylrhodamine ethyl ester perchlorate (TMRE) to measure mitochondrial $\Delta\Psi$ (red image upper right panels). The merged images are shown in the lower right panels. Illustration is from one of three separate preparations. (**b**) Mitochondrial membrane potential using a microplate assay. Please refer to the Methods section for data normalization. Data are means ± s.e., $n = 3$. $^*P < 0.05$. (**c**) The influence of FCCP, pyruvate, N-acetylcysteine (NAC), and combinations on the ATP/ADP ratio. The ATP/ADP ratio was determined in adipocytes following incubation with KRP buffer (adipocytes:KRP buffer 1:3, vol/vol) for 10 min in the presence of FCCP (30 µmol/l), pyruvate (5 mmol/l), pyruvate plus FCCP, NAC (10 mmol/l), or NAC plus FCCP. Data are means ± s.e., $n = 3$. $^*P < 0.05$. (**d**)The effect of pyruvate, NAC, FCCP, or H_2O_2 on ROS levels measured using CM-H_2DCF. ROS levels were measured using CM-DCF at excitation, 490 nm, emission, 529 nm. Cells were first loaded with CM-H_2DCF and then incubated with pyruvate (5 mmol/l), NAC (10 or 20 mmol/l) or H_2O_2 (100 mmol/l) in KRP buffer (5 mmol/l glucose, 1% BSA) as described in methods. Graphs represent experiments that were repeated 5–11 times. Data are means ± s.e. $^*P < 0.05$.

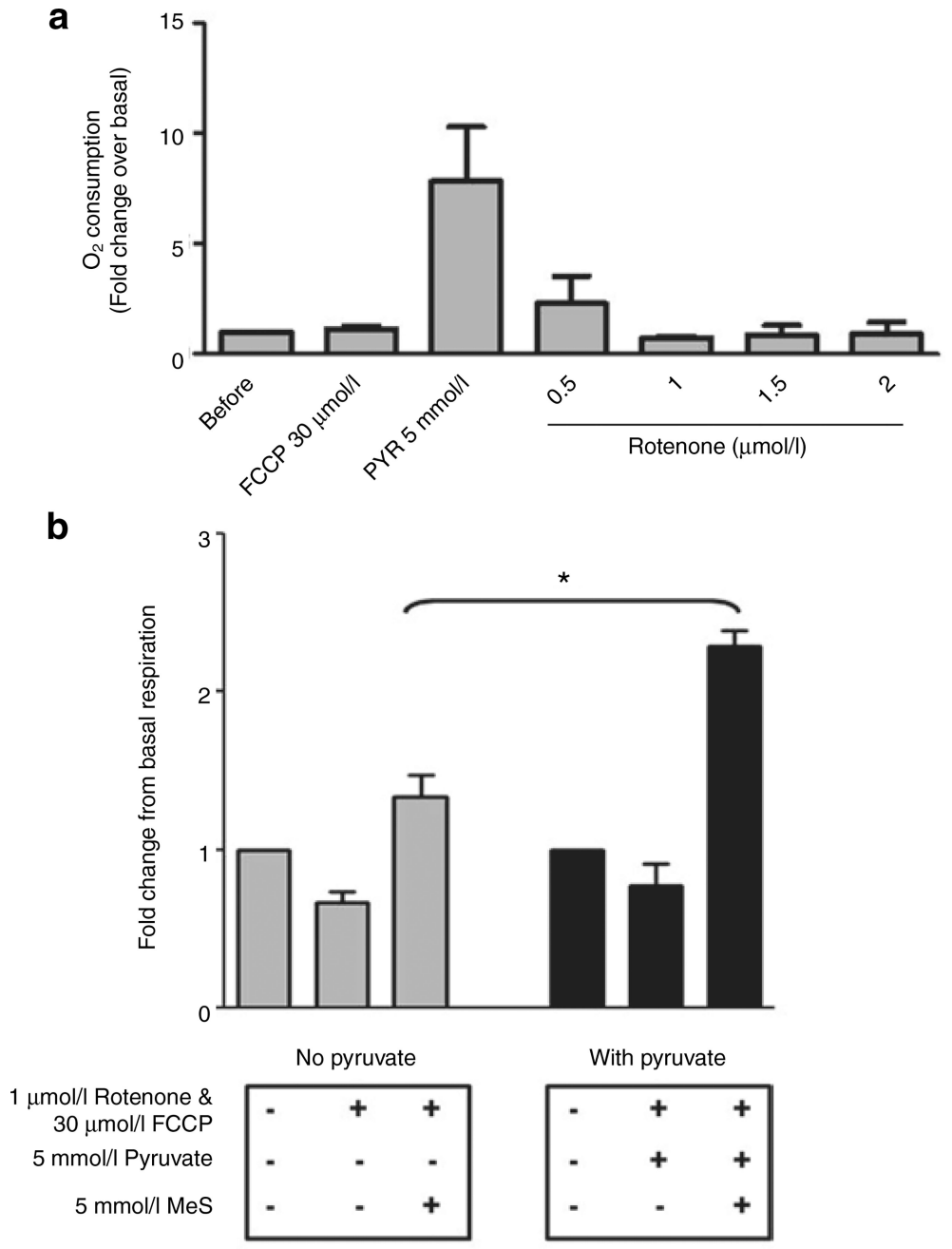

Figure 3.

Effect of inhibiting pyruvate oxidation on respiration with methyl-succinate (MeS) as an alternative substrate. Reagents shown on the x axis were added sequentially and their concentrations are indicated. (**a**) Rotenone dose-dependently inhibited uncoupled O_2 consumption driven by pyruvate. Data shown are fold-change of O_2 consumption rate over basal condition. (**b**) MeS stimulated O_2 consumption in the presence of rotenone and carbonylcyanide p-trifluoromethoxyphenylhydrazone, with (black bar) or without (gray bar) pyruvate. Data shown are relative change of O_2 consumption rate from basal respiration. Data are means ± s.e., $n = 3$. *$P < 0.05$.

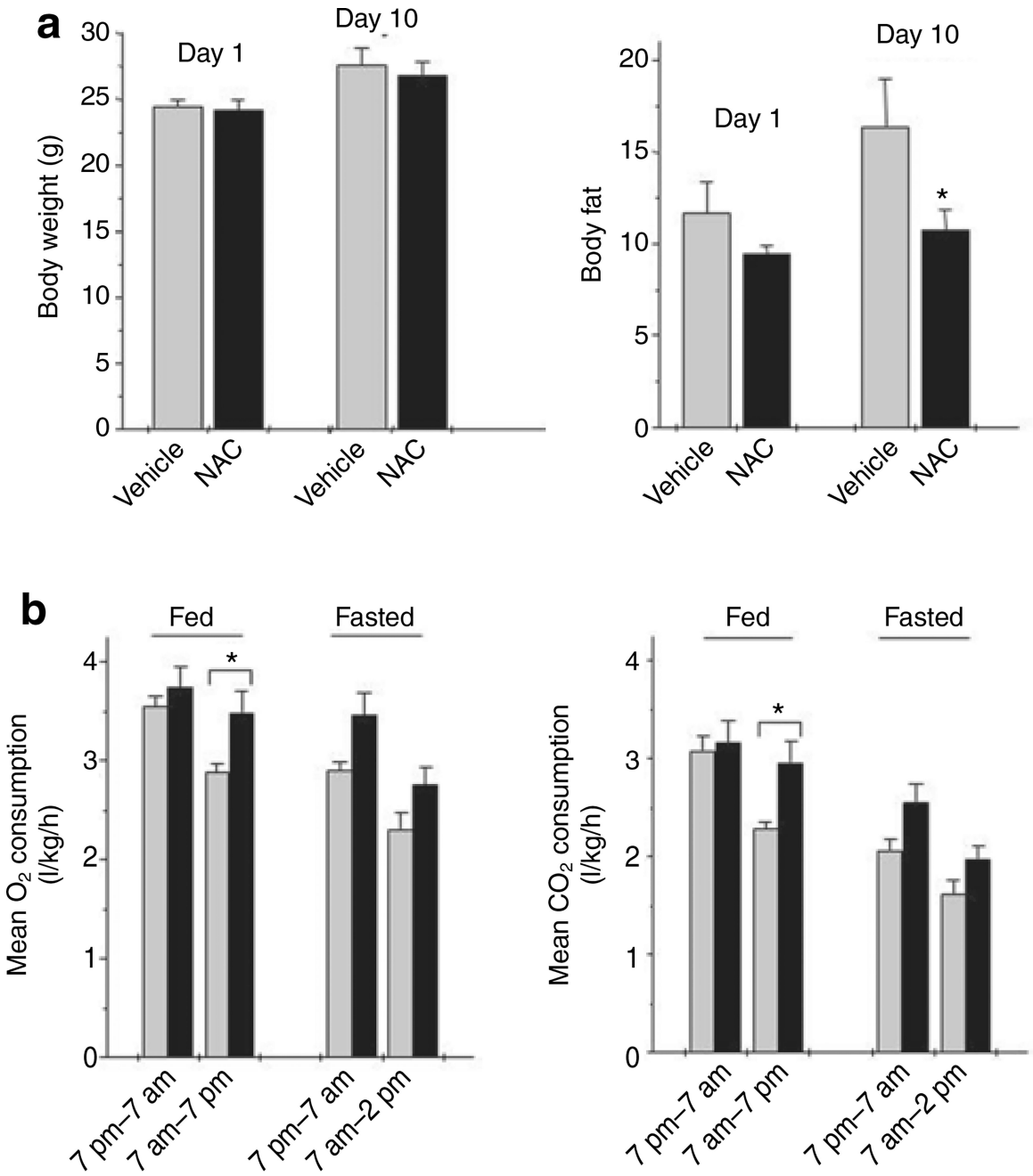

Figure 4.

Effect of N-acetylcysteine (NAC) *in vivo.* (**a**) Body fat and body weight. Postweaning male mice were fed a high-fat diet (35% fat-derived energy). NAC (3 mg/ml) was added to their drinking water and replaced daily (black bars). On days 1 and 10 mice were weighed and analyzed by NMR for fat mass. (**b**) O_2 consumption and CO_2 production. Between day 12 and day 15, mice were analyzed by indirect calorimetry for respiratory rate and CO_2 production. Data are means ± s.e. for four mice. *$P < 0.05$.

Table 1

O_2 consumption of rat white adipocytes with different substrates

	n	O_2 consumption (nmol/min/mg)	*n*	O_2 consumption (nmol/min/mg)
Substrate	**Control**		**FCCP**	
Basal (5 mmol/l Glucose)	65	4.25 ± 0.18	12	3.80 ± 0.43
Methyl-succinate	4	3.37 ± 0.47	4	5.53 ± 1.34
Methyl-succinate/octanoate	3	4.29 ± 1.41	3	5.80 ± 1.83
Acetate	3	7.48 ± 1.95	3	5.20 ± 1.36
Glutamine	3	4.23 ± 1.37	3	4.74 ± 0.96
Octanoate	3	4.77 ± 1.53	3	8.28 ± 2.66
Glutamine/octanoate	3	4.22 ± 0.87	3	3.99 ± 0.98
Malate	3	4.37 ± 1.50	3	6.42 ± 2.30
Lactate	3	4.69 ± 1.13	3	5.35 ± 1.45
Pyruvate	10	4.48 ± 0.87	15	13.95 ± 1.55

O_2 consumption in intact adipocytes was measured in 1 ml of adipocyte suspension (adipocytes/KRP buffer 1:3, vol/vol), and addition of FCCP (30 μmol/l), octanoate (1 mmol/l), methyl-succinate (5 mmol/l), glutamine (2 mmol/l), acetate (5 mmol/l), lactate (5 mmol/l), malate (5 mmol/l), pyruvate (5 mmol/l), or combinations, as indicated. Data are means ± s.e. of experiments from "*n*" separate preparations.

Table 2

O_2 consumption of isolated mitochondria from rat white adipocytes and liver with different substrates

	O_2 consumption (nmol/mg protein/min)							
	Adipocyte mitochondria				Liver mitochondria			
Substrates	***n***	**State 4**	**State 3**	**State 3/State 4**	***n***	**State 4**	**State 3**	**State 3/State 4**
Succinate	5	84 ± 21	271 ± 79	3.30 ± 0.36	6	22 ± 20	156± 13	7.10 ± 0.28
L-Glutamine plus malate	4	41 ± 11	96 ± 21	2.39 ± 0.12	3	12 ± 0.70	48 ± 13	4.58 ± 0.35
Pyruvate plus malate	4	20 ± 3	159 ± 39	7.91 ± 0.58	5	15 ± 2.68	49 ± 13	3.15 ± 0.27

O_2 consumption was measured continuously following sequential addition of substrate (succinate (5 mmol/l), or pyruvate (5 mmol/l) or glutamine (5 mmol/l) plus malate (1 mmol/l) and ADP (0.2 mmol/l). State 4 O_2 consumption reflects O_2 consumption without and State 3, with ADP added. Data are means ± s.e. of "*n*" experiments from separate preparations.